

A Brief Summary of Femtosecond Laser Induced Filamentation

Physics 568- Nonlinear Optics Sp. 2007

Instructor: Dr. Sheik-Bahae

Brook Jilek and Nathan D. Zamoski

Abstract—This research paper will discuss femtosecond induced filamentation.

Index Terms— Filamentation, Nonlinear Refractive Index, Nonlinear wave propagation, Kerr effect, and the Nonlinear Schrödinger Equation (NLSE)

I. INTRODUCTION

WHEN intense laser beams propagate through a medium, the index of refraction of the medium is modified by the optical Kerr effect. The new index of refraction, n , can be described by the equation $n = n_0 + n_2 I$ where n_0 is the nominal linear index of refraction, n_2 is the nonlinear Kerr coefficient, and I is the intensity of the laser beam. A positive value of n_2 leads to self-focusing of the beam where as a negative value lead to de-focusing. If the beam power is sufficiently high, the higher intensities caused by the self-focusing of the beam will ionize atoms in the medium, creating a plasma. This plasma causes a dispersive effect that counteracts the self-focusing. When the two effects shown in Figure 1 exactly counter each other, the beam will propagate without diverging for distances much longer than the Rayleigh range of the laser. The thin channel of plasma created is called a filament.

Filaments can occur when the power of the incident beam exceeds the critical power, P_{cr} , given by the following equation [1].

$$P_{cr} = \frac{\pi 0.61^2 \lambda_o}{8 n_0 n_2} \quad \text{Eq. 1}$$

Filaments are ~100 microns in diameter, have electron densities of 10^{16} - 10^{17} cm^{-3} , peak intensities of 10^{13} - 10^{14} W/cm^2 and can be hundreds of meters long. [2]. When laser intensities greatly exceed the critical power, small fluctuations in the intensity of the beam cause multiple filaments to form, each carrying a power close to the critical power [3]. The intensity profile of the incident beam and its power are the principal criteria for determining the number and shapes of the filaments formed. Filaments have found uses in remote sensing, controlling electrical discharges, the characterization of the dispersive properties of nonlinear media, and the generation attosecond extreme ultraviolet (XUV) pulses.

Mechanism for channel formation

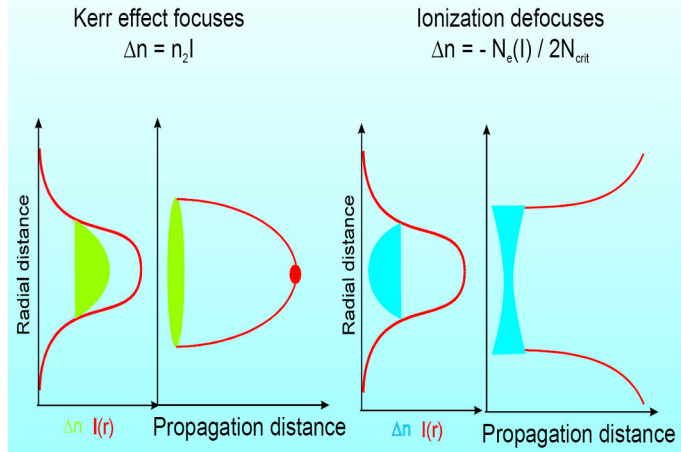


Figure 1, adopted from [4]. Kerr lensing is balanced by defocusing from ionization.

This paper will discuss the following topics. In section II filament collapse dynamics will be discussed with experimental and theoretical validation. In section III we will discuss some applications of filamentation.

II. FILAMENT COLLAPSE DYNAMICS

Braun [5], first studied filamentation in air produced by 100fs, 10mJ pulses in 1995. Since that time there has been growing interest in nonlinear wave collapse dynamics from femtosecond pulses which lead to filamentation in Kerr media and the resulting supercontinuum generation. Several researchers [1-11] have been performing numerical and experimental studies to better explain the complex coupling between the spatial and temporal process which are governed by the 2-D nonlinear Schrödinger equation (NLSE).

The 2-D NSLE is given by the following equation 2 [1]. It describes the self-action affects that the pulse induces upon itself when propagating a Kerr media.

$$\frac{dA}{dz} = \frac{i}{2k_o} \nabla_T^2 A - i \frac{k_2}{2} \frac{dA^2}{dt^2} + i\gamma_1 |A|^2 A - 2\gamma_1 \frac{d(|A|^2 A)}{dt} - \frac{\beta^M |A|^{2M-2} A}{2}$$

$$\text{Where...} \gamma_1 = \frac{6\pi\omega_o}{c} \chi^{(3)}$$

$$\text{Where...} \chi^{(3)} = \frac{n_2 n_0}{3\pi}$$

Eq. 2 ↑

Where A is the envelope amplitude of the wave packet of the carrier frequency ω_0 , ∇_T^2 is the Laplace operator which accounts for diffraction, c is the speed of light, n_0 and n_2 are the linear and nonlinear refractive indexes respectively, k_2 accounts for group velocity dispersion (GVD), $\chi^{(3)}$ is the 3rd order nonlinear susceptibility, the term $|A|^2 A$ accounts for self-phase modulation (SPM) and the term $\frac{d}{dt}(|A|^2 A)$ accounts for nonlinear shock and self-steepening of the pulse. SPM leads to symmetric spectral broadening around ω_0 , whereas the self steepening term that leads to optical shock results in asymmetric spectral broadening of the pulse. Self-steepening can be explained by the intensity-dependence of the group velocity [1]. As the intensity of a pulse increases from its leading edge to the pulse center, the index of refraction increases as well (assuming $n_2 > 0$), causing the higher intensity center of the pulse to become shifted towards the trailing edge of the pulse. This can result in an optical shock leading to supercontinuum generation. The last term on the right side of equation 2 accounts for multiphoton absorption (MPA) and nonlinear losses. M is the order of the process and β is the MPA coefficient. This term leads to filamentation arrest i.e. it reduces power in the filament and eventually stops the filament.

In general equation 2 is a nonlinear partial differential equation that must use numerical methods to solve for the A . One such numerical method is the Split Step Fourier Method (SSFM) and the other is the inverse scattering method. Refer to Agrawal [6] for a complete description on how to implement the SSFM.

A remarkable prediction of the 2-D NLSE is that the spatial profile of the beams evolves into universal, self-similar, circular symmetric shape regardless of the shape of the initial beam. For the NLSE, this profile is known as the Townes profile (TP), as shown in figure 2 [7].

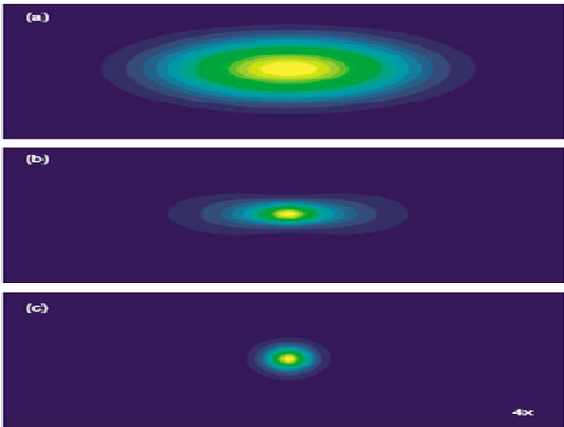


Figure 2 Adopted from [7]. The propagation of an elliptically shaped input (a) is simulated. As the beam propagates (b) it self focuses, and a circularly symmetric TP is formed on the axis and (c) as beam collapses. Part (c) has a 4 x magnification to show more detail.

The TP corresponds to the unstable solution in which nonlinear focusing and diffraction precisely balance each

other, and the beam maintains a constant profile [7]. A crucial property of the TP is that the power contained within the collapsing portion of the beam is always precisely equal to the critical power for self-focusing.

It has been established that as a Gaussian beam approaches the point of collapse, the beam evolves to the TP [8]. Recent theoretical work by Fibich [9] involving Super-Gaussian (SG) beams has shown that there is another possible solution to the 2-D NLSE, in which SG beams of high power ($\sim 10P_{cr}$) collapse to a self-similar ring shaped profile called the G-profile. At powers $\sim P_{cr}$ or a little above, SG beams behave like Gaussian profiles and collapse to the TP. However, in the presence of noise, modulational instability causes beams of any profile to collapse into multiple filaments, each conveying a power close to $\pi^2 P_{cr}/4$ [3].

SG beams undergo multiple filamentation at much lower powers ($P \sim 10P_{cr}$) than with Gaussian beams ($P \gg 100P_{cr}$). Observe in Figure 2, the profiles of the solution to the NLSE for SG beams with no noise and propagation distance ζ . In figure 2a the $P=5P_{cr}$ and the SG beam collapses to the TP, while in figure 2b $P=10P_{cr}$ and the SG beam collapses to a ring profile.

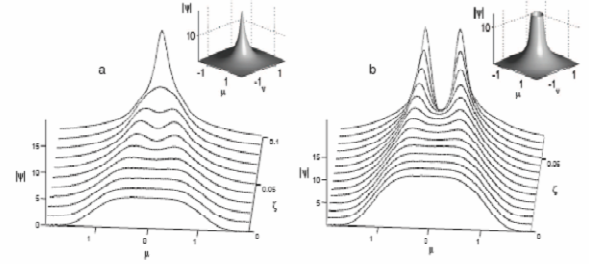


Figure 3. Adopted from [8]. Profiles of the solutions to the NLSE for a SG beam at two input powers. (a) $P=5P_{cr}$ and (b) $P=10P_{cr}$

Observe in Figure 4, that when a 5% amplitude noise is applied the SG pulse with $P=20P_{cr}$ the pulse undergoes multiple filamentation after it propagates from $\zeta = 0$ to a normalized distance of $\zeta = 0.05$, where $\zeta = z/2 * L_{df}$ and L_{df} is the diffraction length. It was observed from simulations that the number of filaments formed from a SG beam is proportional to the square root of the input power.

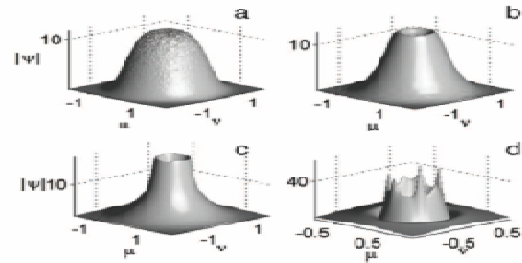


Figure 4. adopted from [8]. Solutions to the NLSE with a SG input beam with 5% amplitude noise and input power of $20P_{cr}$ at distances (a) $\zeta=0.0$, (b) $\zeta=0.025$ (c) $\zeta=0.0375$ and (d) $\zeta=0.05$

As filaments propagate, they can interact with each other or even merge into one depending on their spatial separation and

power [3]. Filaments that are very close to each other have strongly coupled transverse dynamics. When two filaments are near each other but not propagating exactly parallel to each other, it can become energetically favorable for the two beams to coalesce, as in Figure 5a below. To coalesce into one filament, the two initial filaments must each have a power less than about $1.35 \cdot P_{cr}$ and be separated by less than a critical distance defined by $\sqrt{10}$ times the filament waist size [3]. If the power contained in each filament is more than this, the filaments will not coalesce into one filament, but will combine in a stable oscillating mode, as seen in Figure 5b. But when the distance between filaments becomes greater than the critical distance, the filaments will maintain their soliton propagation over appreciable distances, as in Figure 5c. With the high intensities associated with filamentation, multi-photon absorption (MPA) becomes an important process that continually decreases the soliton power until the dispersive effects of ionization win out and the solution to the NLSE is no longer valid. Figure 5d shows the effect of MPA on the propagation of filaments. After MPA has reduced the power contained in the filament to below P_{cr} , the beam starts to disperse. After propagating some distance the two disperse beams overlap and the intensity once again becomes great enough for a new filament to be produced.

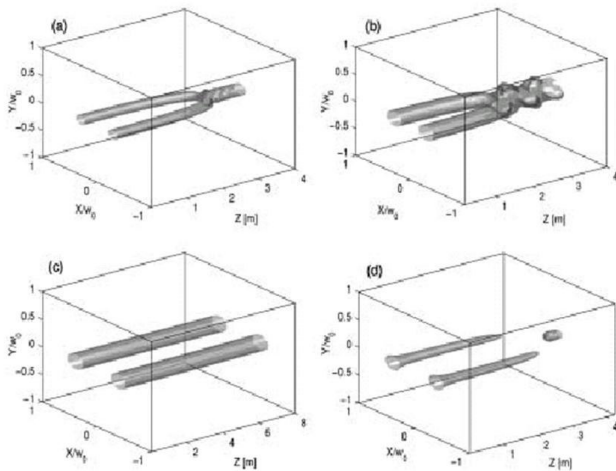


Figure 5 as adopted from [3] a.) Two solitons of equal power separated by .6 mm fuse into one filament, MPA neglected b.) Two solitons of greater power than in a.) with same separation oscillate together, MPA neglected c.) Solitons with same power as in b.) but separation increased to .8 mm do not interact, MPA neglected. d.) Same power and separation as in c.) but with MPA. Filaments disperse and then form a new filament.

Figure 6 shows a 3D simulation by Bergé of beam collapse and multiple filamentation in air as a function of propagation distance. In this simulation, amplitude noise in the input beam causes hot spots in the beam to change the local index of refraction and seeds the formation of multiple filaments.

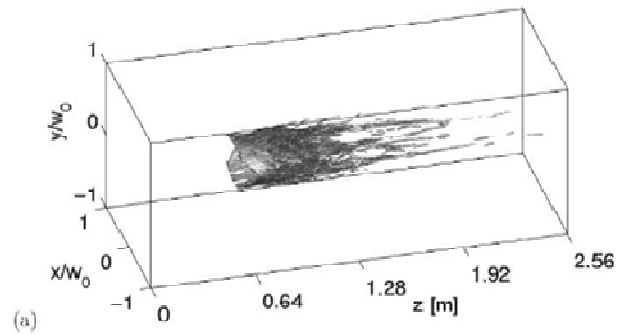


Figure 6. adopted from [3]. A full 3D simulation of 85 fs Gaussian beam with 10% amplitude noise.

This collapse of SG beams into multiple filaments has been observed in experiments performed by Bergé [3] and Grow [8]. In experiments conducted by Grow [8], 90 fs, 800 nm pulses from a Ti:sapphire amplifier with a repetition rate of 1kHz were sent through the experimental set-up show in figure 7 and focused into a cell of deionized water. The beam shape was controlled by a spatial light modulator.

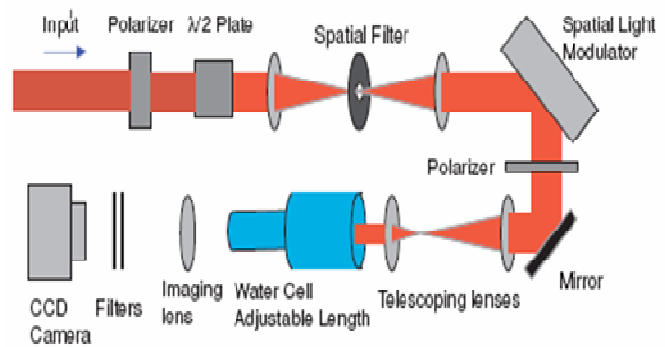


Figure 7 adopted from [8]. Schematic of experimental set-up used to observe beam collapse.

In one of the many experiments performed with this set up, the length of the water cell was kept constant at 10cm and the input power (pulse energy) was increased just to the point below supercontinuum generation while monitoring for filamentation by using imaging optics and CCD camera.

The results of these experiments are in good agreement with the theoretical simulations. Figure 8 shows the dependence of input (a, b, c) SG collapse profiles as a function of input power and the corresponding output profiles (d, e, f). Observe that as pulse energy (beam power) is increased the SG beam will collapse to a TP (e, f). As beam power is further increased ($P \gg 10 P_{cr}$) SG beams collapse to a ring profile figure 8 (f) with multiple filaments. In this experiment, the diameter of the SG beam was increased in b and c so not to damage the SLM.

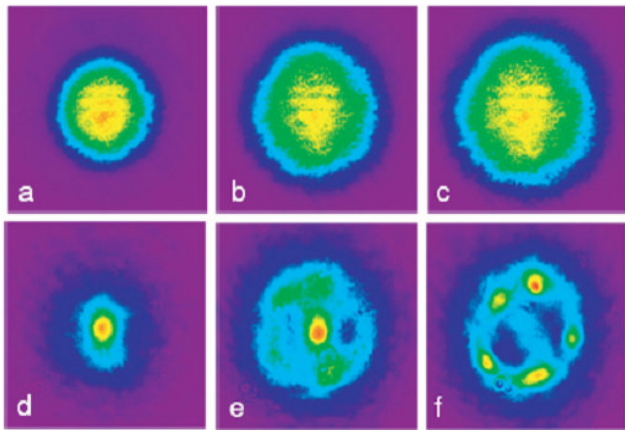


Figure 8 adopted from [8]. Input super-gaussian beams (a-c) for increasing energy and the corresponding output profiles (d-f) just before supercontinuum threshold in a 10cm water cell. (d) $E=4.2\mu\text{J}$, (e) $E=9.1\mu\text{J}$ and (f) $E=17.5\mu\text{J}$

III. APPLICATIONS

Some applications of laser induced filamentation include the following: supercontinuum generation (SCG) for white light lidar and the detection of biological agents, triggering electrical discharges, determining dispersion landscape of materials through conical emission and generation of attosecond pulses.

Since filaments are guided channels of conducting plasma, it has been suggested that filaments can be used to trigger electrical discharges and guide them along the laser beam. The ability to channel lightning away from sensitive areas like nuclear, biological, and chemical plants and airports has been the prime impetus for this research. Although the technical challenges of triggering lightning in rainy weather are great, Rodriguez [10] has demonstrated that filaments can be used to trigger and guide electrical discharges over several meters. Figure 7 below describes the experimental setup and results.

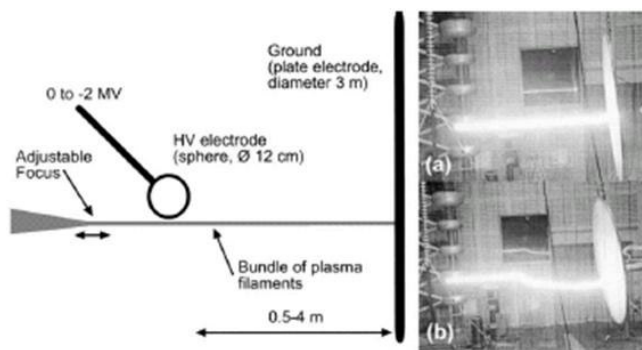


Figure 7. Adopted from [10]. The laser filament passes close by the spherical electrode, exciting the discharge. In a.) the filament extends all the way to the ground plate and the discharge is directed all the way from the electrode to the ground plate. In b.) the filament does not extend all the way to the ground plate, so the discharge is only partially directed.

In another application, filaments are generated in hollow core gas filled fibers and the spectrally broadened spectrum is

compressed to a few optical cycles to conduct attosecond (10^{-18}s) physics experiments [11] [12] [13]. Such experiments are used to conduct attosecond time domain spectroscopy and are used to generate attosecond extreme ultraviolet (XUV) pulses.

One of the main advantages of using gas filled fibers over photonic crystal fibers to generate SC is that higher power (μJ to mJ instead of nJ) white light can be generated. In addition to low loss and high spatial beam quality, gas filled fibers offer the following advantages, 1) purely electronic 3rd order nonlinearity, 2) control of the nonlinearity strength by gas type and pressure, 3) high threshold intensity for multiphoton ionization particularly for fs pulses[11].

IV. CONCLUSION

We have shown that nonlinear wave collapse leading to filamentation of femtosecond pulses is a complex process governed by the NSLE. The physical mechanism leading to filamentation is the balance of Kerr self-focusing and plasma generation which tends to defocus the laser beam. We have also shown that filamentation is highly dependent upon beam power and pulse shape. Filamentation has been widely studied and for the most part can be explained through theoretical models and validated with experiments. However, research is still being conducted to further explain and exploit this complex spatial-temporal process.

REFERENCES

- [1] Boyd, Robert W., Nonlinear Optics, 2nd edition, 317-323 (2003)
- [2] Rohwetter, Ph., et al., Spectrochimica Acta Part B, 60, 1025-1033 (2005)
- [3] Bergé, L., et al., Physica Scripta T107, 135-140 (2004)
- [4] <http://pclasim47.univ-lyon1.fr/teramobile.html>
- [5] A. Braun et al. Opt. Lett. Vol.20 No. 73, 1995
- [6] Agrawal, Nonlinear Fiber Optics, 3rd edition
- [7] K.D. Koll and A.L Gaeta, Physical Review Letters, Vol. 90, No. 20 2003
- [8] T.D. Grow, et al. Optics Express, VOL.14 No. 12 2006
- [9] Fibich, et al., Physica D 211,193-220 (2005)
- [10] Rodriguez, M., et al. Optics Letters Vol. 27, No.9 (2002)
- [11] M. Nisoli, et al. Appl. Phys. Lett. 68 (20),1996
- [12] M. Nisoli, et al. IEEE. Journal of Selected Topics in Quantum Electronics, Vol.4, No. 2 1998
- [13] M. Nisoli, et al. Appl. Phys. B. 75, 601-604 (2002)